Journal of Applied Sciences

ISSN 1812-5654

science alert

ANSInet
an open access publisher
http://ansinet.com

Journal of Applied Sciences 9 (20): 3752-3757, 2009
ISSN 1812-5654

A Study of Winglet and Aerodynamic Interferences in 3-D Viscous Flow around a Flying-Boat in Ground Effect

H. Afshar and M.M. Alishahi
Department of Mechanical Engineering, School of Engineering, Shiraz University, Shiraz, Iran

Abstract: In this study, the flow field about a complete flying-boat in ground effect is resolved. The influences of using winglet in ground and out of ground effects are compared and it is shown that ground affects this influence to a large extent. It is also shown that with careful shaping of the body and using a step underneath the body a propulsive force can be produced in vicinity of the ground. However, this causes an increase in drag force in free flight.

Key words: WIG, CFD, ground effect, aerodynamics, parallel processing

INTRODUCTION

Aerodynamic design has always been a timely and expensive process specially when using experimental tools and in the final stages of design, refining the details of the configuration. Also, taking advantage of aerodynamic interferences of different components involves setting up various models which increases again the financial burden. CFD simulations with large number of grid points are a real competent for experiment if it is carefully set up. This procedure is followed in this study to simulate the aerodynamic interferences of parts of a flying boat in the vicinity of the ground.

Flying vehicles in vicinity of ground (wing in ground effect, WIG) are more efficient aerodynamically, Kornev and Matveev (2003) and have consequently attracted the interest of designers. It has long been recognised that flight close to a boundary surface is more aerodynamically efficient than flight in the freestream. This has led to the design and construction of craft specifically intended to operate close to the ground and fly in ground effect. A great range of Wing in Ground (WIGs) effect craft have been manufactured ranging from 2 seat recreational vehicles to 500 tonne warcraft. In addition to the aerial transportation in ground effect, there has been interest on high speed trains moving on air gap (Cho *et al*., 2001; Kohama and Watanable, 1998; Moon *et al*., 2005). Ground affects lift and other aerodynamic forces to a large extent, (Kim and Geropp, 1998; Zhang *et al*., 2004) and these effects come through a complicated process of deformation and displacement of vortices (Florent *et al*., 2000; Zhang and Zerihan, 2003; Engels *et al*., 2004).

Fig. 1: A flying-boat

Recent studies of ground effect are limited to two-dimensional cases or three dimensional flows around some specific components (Kim and Geropp, 1998; Zhu *et al*., 2002). The complex configuration of flying boat (Fig. 1) can only be properly modeled using multi-blocked structured grid that is used in this study.

GRID GENERATION

Even small experience in solving complicated flow problems warrants that a good grid comprises half of what is required for a good solution. Due to the complexity of the configuration, Fig. 1 and possible separation of the viscous flow in various regions, application of a structured grid especially close to boundaries is preferred to the unstructured grid. The properties of a good grid includes uniformity, smoothness and near orthogonality to boundaries (Zhu *et al*., 2002) and no single-block grid can provide all of these simultaneously, therefore,

Corresponding Author: Hossein Afshar, No. 605, Imam Khomeini Ave., Between Khosh and Ghasre Dasht, Tehran, Iran
Tel: +989126764193

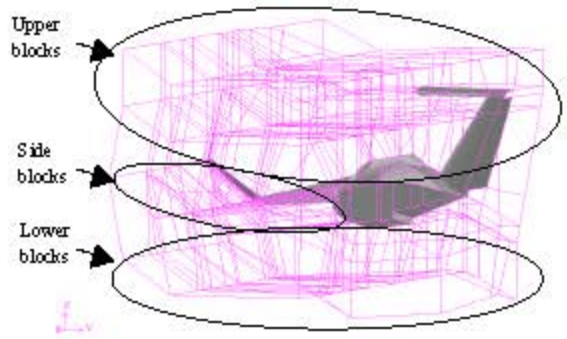

Fig. 2: Different blocks in vicinity of the body used for structured grid generation

multi-block grid is applied in this study (Radespiel, 1987; Rakowitz and Eisfeld, 2003). However, at the interface of different blocks discontinuities in position and slope of grid lines should be avoided in order to resolve all the details of the flow and maintain a high convergence rate of the solution at the same time (Jie and Jou, 2008; Martins *et al*., 2005).

The configuration properties (Fig. 1) include swept back vertical tail, high taper ratio wing with swept forward trailing edge among the others. Therefore, three main blocks, about upper-body, lower-body and side-body plus wing choosed and divided into smaller blocks of 800 altogether (Fig. 2).

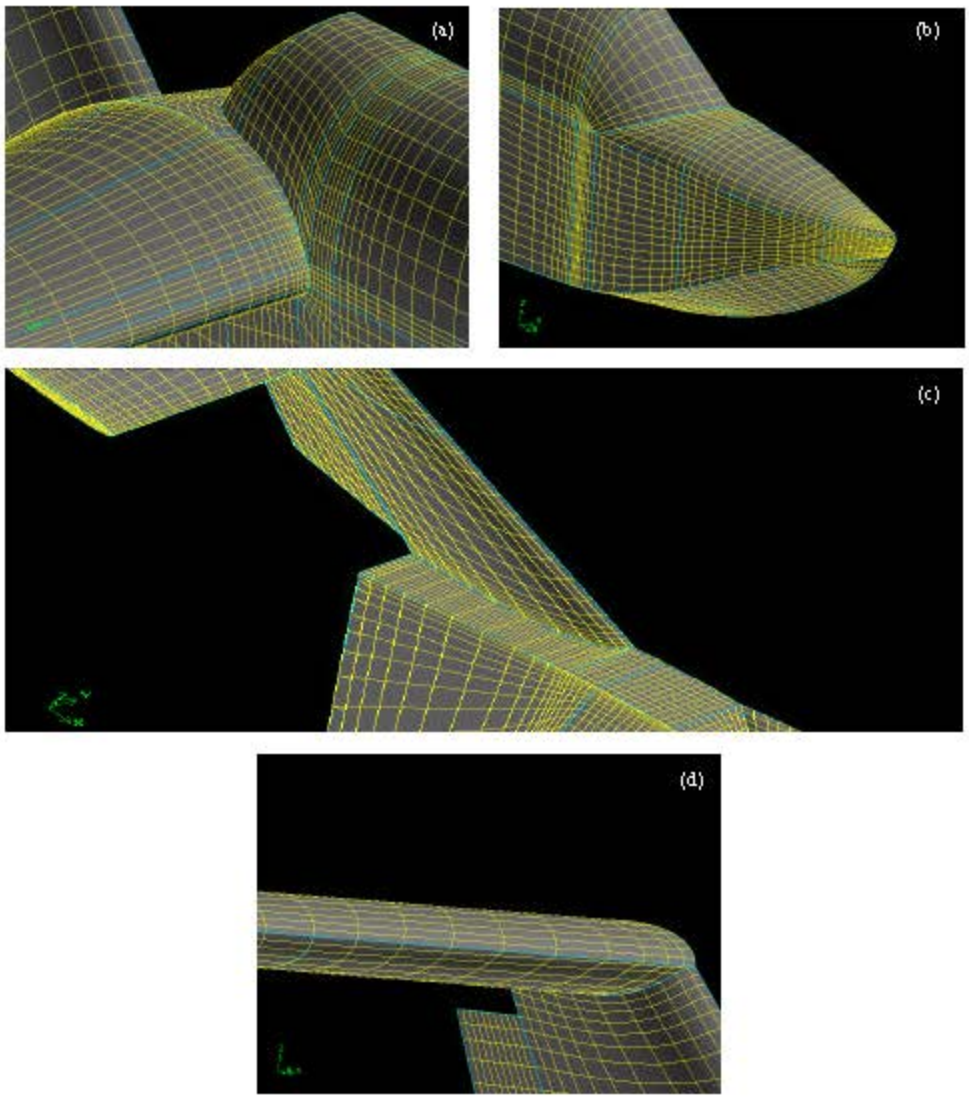

Fig. 3: (a) Structured grid in the junction of fuselage and wing, (b) Structured grid in nose and canopy), (c) structured grid at the junction of wing trailing edge, vertical tail and fuselage and (d) structured grid at the junction of vertical and horizontal tails

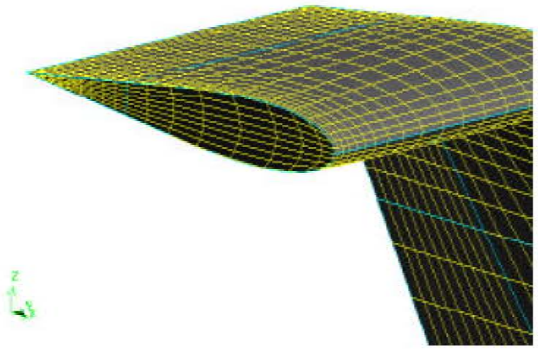

Fig. 4: Unstructured grid on the tip of tail

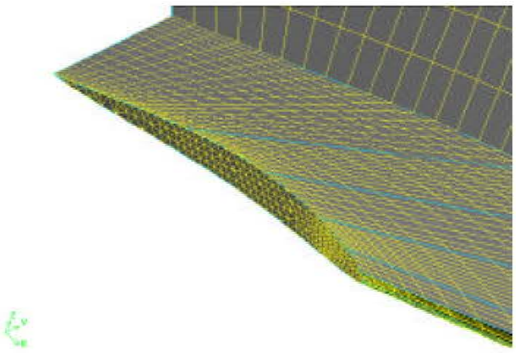

Fig. 5: Unstructured grid on the tip of winglet

These large numbers of blocks are used to maintain smooth transition e.g., when connecting grids from swept forward trailing edge of the wing to the horizontal tail. Also some of the blocks are there to keep the near orthogonality of grids to the boundary. The resulted grid is smooth and uniform (Fig. 3a-d).

In few regions of the flow field use of unstructured grid is inevitable. Although, these regions are small and quite few, this flexibility warrants the grid quality in more important regions. These regions contain tips of wing, winglet, control surfaces and horizontal tail (Fig. 4, 5). Proper distribution of grid points on different edges provides the required control of the uniformity and smoothness.

GOVERNING EQUATIONS AND BOUNDARY CONDITIONS

Reynolds averaged, incompressible, steady-state Navier-Stokes equations are:

$$\frac{\partial u}{\partial x}+\frac{\partial v}{\partial y}+\frac{\partial w}{\partial z}=0$$

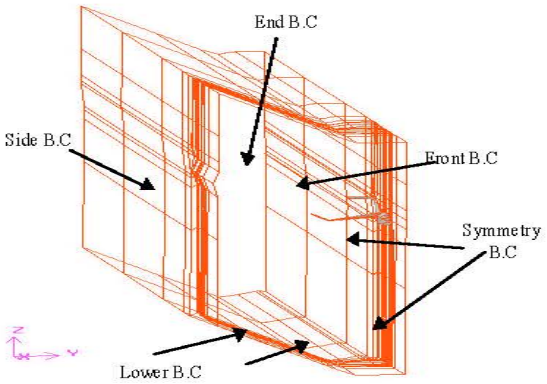

Fig. 6: Different boundary conditions

$$\rho\nabla.(\vec{v}.\vec{v})=-\nabla p+\nabla.(\bar{\bar{\tau}})$$

where, u, v and w are velocity components of velocity vector, $\vec{v}$, in x, y and z directions, respectively. The p and ρ are pressure and density and τ_{ij} are different components of stress tensors as:

$$\bar{\bar{\tau}}=(\mu+\mu_T)(\nabla\vec{v}+\nabla\vec{v}^T)$$

Two equation k-ε turbulence modeling is used to determine μ_t in terms of kinetic energy, k and dissipation, ε as:

$$\rho\frac{\partial}{\partial x_i}(ku_i)=\frac{\partial}{\partial x_j}\left[\left(\mu+\frac{\mu_t}{\sigma_1}\right)\frac{\partial k}{\partial x_j}\right]+G-\rho\varepsilon$$

$$\rho\frac{\partial}{\partial x_i}(\varepsilon u_i)=\frac{\partial}{\partial x_j}\left[\left(\mu+\frac{\mu_t}{\sigma_\varepsilon}\right)\frac{\partial \varepsilon}{\partial x_j}\right]+C_1\frac{\varepsilon}{k}G-C_2\rho\frac{\varepsilon^2}{k}$$

$$\mu_t=\rho C_\mu\frac{k^2}{\varepsilon}$$

Figure 6 shows half of the airplane and the domain for an angle of attack problem. As can be shown in Fig. 6, on some of the boundary planes velocity and turbulent properties are defined and on the downstream plane pressure is set. Water surface is modeled as a planar surface with zero shear stress. In this way of modeling, the water surface, the effect of air flow on free surface deformation and wave production is neglected.

NUMERICAL ALGORITHM

As mentioned before, simple algorithm along with the first order upwind method is used to discretize the momentum and the mass conservation equations.

Table 1: Grid study results and aerodynamic coefficients

Grid count	Cl	Cd	Error (%) (Cl)	Error (%) (Cd)
1.5 million	0.824	0.107	5.614	1.289
4 million	0.784	0.108	0.449	2.417
6.5 million	0.780	0.106	------	-------

Since, this is a quite known procedure no further explanation is provided.

A grid study including 1.5, 4 and 6.5 million grid points carried out and the results are shown in Table 1. In Table 1, lift and drag coefficients, lift over drag and the relevant errors are presented. The error is the relative percent error in results with respect to the final row. It is seen that both 4.5 and 6.5 million grid points are fine enough to provide the coefficients with acceptable error. However, y+, i.e., the normalized non-dimensional distance to the wall is only within the acceptable range for the last grid case. Since, the logarithmic velocity profile is applied in the boundary region the proper range of y+ for the first grid point should be between 50 and 500. Therefore, the last grid case of Table 1 is used to resolve the following flow fields.

RESULTS

Flow field at zero angle of attack in ground and out of ground effect: When the body is set at zero angle of attack, the wing will be at 8 degrees with respect to the free stream. A comparison of aerodynamic coefficients in ground and out of ground is presented in the followings. In free flight, the lift, drag and pitching moment coefficients about the leading edge are 0.564, 0.098 and 0.089, respectively. When the flight height (height of the wing trailing edge above ground) is 30% of the root chord, these coefficients change to 0.693, 0.0967 and 0.1383. This indicates a noticeable. i.e., 23% increase in lift and 25% increase of aerodynamic efficiency or lift/drag which is expectable. However, the drastic increase in pitching moment with flight height, i.e., 55% needs more explanation as follows. Although, the symmetric airfoil of horizontal tail is set at zero degrees of angle of attack, it produces a coefficient of lift equal to -0.0569 which is 10% of the total of lift in free flight condition. This downward force is mainly caused by the interference of the main wing to a large extent and to the vertical tail to a lesser extent. When the boat flies close to the ground at the mentioned height the horizontal tail tends to produce positive lift, due to ground, which results in a less net negative lift, i.e., a coefficient of lift equal to -0.0476 or 6.8% of the total lift. This noticeable change in lift of horizontal tail produces due amount of change in pitching moment coefficient during take-off.

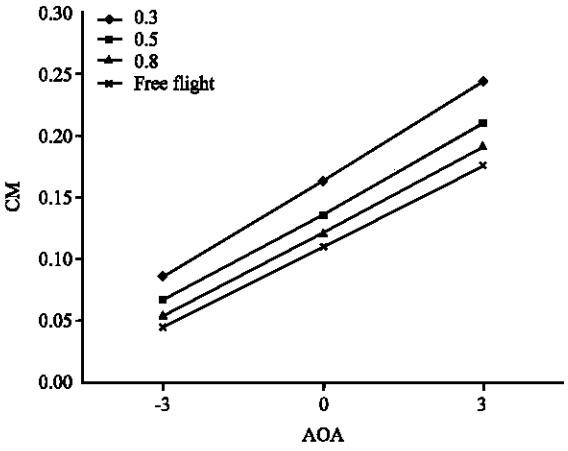

Fig. 7: Variation of CM versus AOA and distance from ground

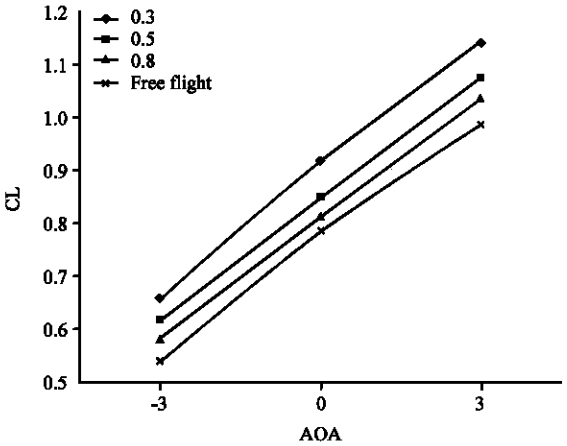

Fig. 8: Variation of CL versus AOA and distance from ground

The next important effect of ground is on the body drag. The body has a boat-tail shape from its maximum cross section tapered to the end. This part produces a propulsive force (negative drag) in free flight. In addition to this part, the same effect is generated by a step located in the lower part of the body. It is interesting that step drag force in free flight becomes a propulsive component in vicinity of the ground and hence contributes to higher lift/drag in ground effect. The high setting of wing at 8 degrees angle of attack enhances this effect by generating a high pressure area around body and beneath the wing. The overall effects of ground on various aerodynamic coefficients with angle of attack are shown in Fig. 7-10. The same trend is seen in Fig. 7-10; however, the nonlinearity o f lift variation with angle of attack even in 6 degrees range of variation is noticeable (Fig. 10). This is

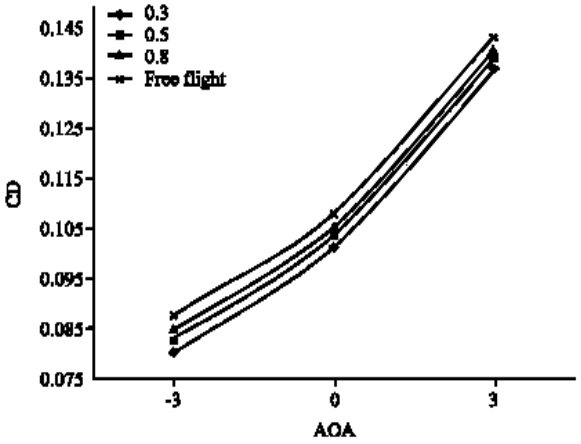

Fig. 9: Variation of CD versus AOA and distance from ground

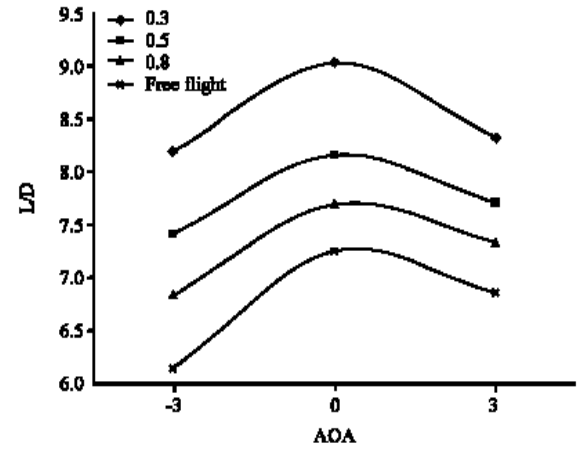

Fig. 10: Variation of L/D versus AOA and distance from ground

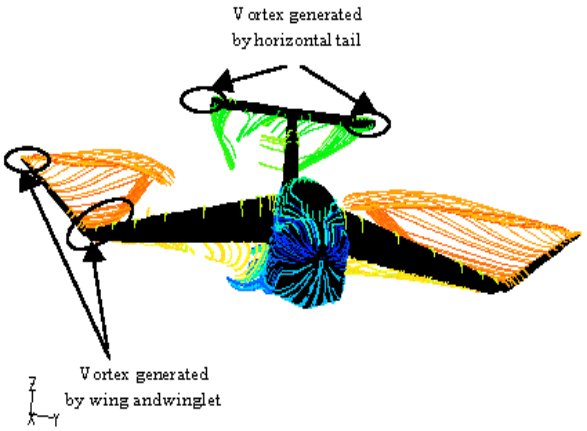

Fig. 11: Path lines of a flying boat

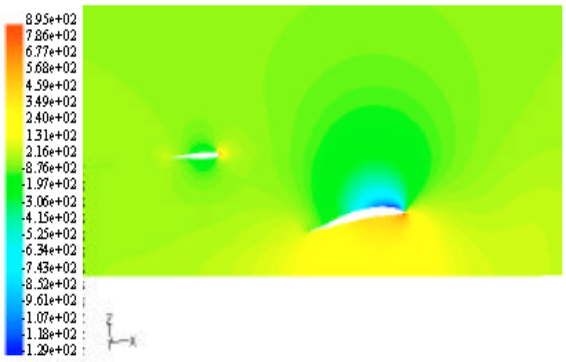

Fig. 12: Pressure distribution in cross section with 15 cm distance from body

mainly due to the interaction of vortices coming off from wing tips and other parts of the configuration, explained in the followings.

Comparison between the experimental lift and drag of a flying boat that is available in high performance Computer Center of Shiraz University (HPCC) and the numeric results of this study is done. Experimental lift and drag coefficients for the case h/c = 0.3 are 1.1 and 0.158, respectively which shows a deflection of 3.6 and 15.6% according to Fig. 8 and 9. This deflection is in acceptable range for numerical calculations.

The effect of winglet in ground and out-of-ground effect: The cases discussed up to now had no winglet. In Fig. 11, the path lines from different parts of the whole configuration including winglet are shown. The interaction of vortices with each other and with the main flow field is quite strong.

Addition of winglet to the configuration in free flight increase the lift coefficient by 36%, the pitching moment coefficient by 22% and lift over drag by 2.8%. It is interesting that the winglet increases the downward lift of the horizontal tail by 14%. This increase in negative lift is due to the effect of stronger tip vortices and the downwash induced by vortices, (Fig. 11). Addition of winglet in presence of ground increases the lift by 32%, pitching moment by 17% and aerodynamic efficiency by 26%. These numbers show that the winglet influence reduces as the flying-boat decreases its height.

Figure 12 and 13 show the pressure contours at two span wise sections of wing and horizontal tail. The pressure underneath the horizontal tail is negative due to wing effect and this pressure change is enhanced by the presence of the vertical tail. This increase is due to the vertical tail effect. In overall, if the flying-boat increases

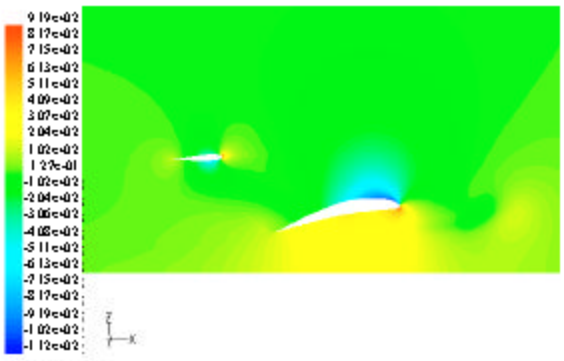

Fig. 13: Pressure distribution in cross section with 1 m distance from body

its height above the ground a nose up pitching moment would apply on the plane due to increased negative tail lift which is mainly due to interferences.

CONCLUSION

Configuration tuning would take the best advantage of ground effect in increasing lift and aerodynamic efficiency. Strong interference of wing and the horizontal tail produces a large pitching moment amplified in ground effect. Winglet has a broad effect on performance of all parts, even on the canopy lift at upstream (not mentioned in the text). However, the main effect would be to increase the lift and aerodynamic efficiency, which is more pronounced in free flight than in ground presence. The interference of wing and vertical tail on horizontal tail is a net downward force on tail. As this force increases with increasing the height a nose up moment would assist the take-off.

REFERENCES

Cho, J.S., C.H. Han, Y.J. Moon and J.H. Beak, 2001. Areodynamic analysis and design of aerolevitation electric vehicle. AIAA CP-2435-AIAA Applied Aerodynamics Conference, 19th, Anaheim, CA, June 11-14. http://www.aiaa.org/content.cfm?pageid=406&gTable=mtgpaper&gID=20953.

Engels, H., W. Becker and A. Morris, 2004. Implementation of a multi-level optimisation methodology within the e-design of a blended wing body. Aerospace Sci. Technol., 8: 145-153.

Florent, P. and V. Xavier de Saint, 2000. Interaction of wake vortices with the ground. Aerospace Sci. Technol., 4: 239-247.

Jie, L. and Z. Jou, 2008. A structured mesh euler and interactive boundary layer method for wing/body configurations. Chinese J. Aeronautics, 21: 19-27.

Kim, M.S. and D. Geropp, 1998. Experimental investigation of the ground effect on the flow around some two-dimensional bluff bodies with moving-belt technique. J. Wind Eng. Ind. Aerodyn., 74-76: 511-519.

Kohama, Y. and H. Watanable, 1998. Wind tunnel study of the new concept low-emission high speed ground transport system. Proceeding of the 4th KSME-JSME Fluid Engineering Conference, pp: 169-172.

Kornev, N. and K. Matveev, 2003. Complex numerical modeling of dynamic and crashes of wing-in-ground vehicles. 41st Aerospace Sciences Meeting and Exhibit, Reno, Nevada, January 6-9, American Institute of Aeronautics and Astronautics 2003-600, pp: 1-9.

Martins, R., E. Elsholz, S. Barakat and B. Colak, 2005. 3D viscous flow analysis on wing-body-aileron-spoiler configurations. Aerospace Sci. Technol., 9: 476-484.

Moon, Y.J., H. Joon Oh and J. Hee Seo, 2005. Aerodynamic investigation of three-dimentional wings in ground effect for aero-levitation electric vehicle. Aerospace Sci. Technol., 9: 485-494.

Radespiel, R., 1987. Grid generation around wing-body-combinations using a multi-block structured computational domain. DLR-IB 129-87/16, DLR Institute of Design Aerodynamics, 1987.

Rakowitz, M. and B. Eisfeld, 2003. Structured and unstructured computations on the DLR-F4 wing-body configuration. J. Aircraft, 40: 256-264.

Zhang, X. and J. Zerihan, 2003. Off-surface aerodynamic measurements of a wing in ground effect. J. Aircraft, 40: 716-725.

Zhang, X., A. Senior and A. Ruhrmann, 2004. Vortices behind a bluff body with an unswept aft section in ground effect. Int. J. Heat Fluid Flow, 25: 1-9.

Zhu, B., X. Chi and T.I.P. Shih and J.W. Slater, 2002. Computing aerodynamic performance of 2D iced airfoils blocking strategy and convergence rate. AIAA-2002-3049, 20th AIAA Applied Aerodynamics Conference, St. Louis, Missouri, June 24-26, 2002. http://pdf.aiaa.org/preview/CDReadyMAAC02_560/PV2002_3049.pdf.